

Similarities Between Jovian
Decametric and Terrestrial
Kilometric Radiation

by

N. Douglas Hosford

A critical essay submitted in partial fulfillment of the
requirements for the degree of Master of Science
in the Department of Physics and Astronomy
in the Graduate College of
The University of Iowa

July 1973

Chairman: Professor Donald A. Gurnett

ACKNOWLEDGMENTS

I wish to thank Dr. Gurnett for having suggested the topic for the essay and for his advice, encouragement, and very informative discussions.

Thanks are also due Dr. Stanley Shawhan for his helpful advice and suggestions for finding current references to Jovian material.

I wish to thank also Sandy Van Engelenhoven for the typing of this manuscript and other indispensable assistance I have received.

ABSTRACT

Observational evidence concerning Jupiter's decametric radio emission and terrestrial kilometric emission is reviewed. Some of the more probable theories for each emission are briefly outlined and tests suggested.

The question "Can Jovian decametric radiation and terrestrial kilometric emission have similar generating mechanisms?" is discussed. It is concluded that the two phenomena may be generated close to the electron gyrofrequency. The conditions necessary for terrestrial kilometric radiation generation are outlined.

TABLE OF CONTENTS

	Page
TABLE OF TABLES	vii
TABLE OF FIGURES	viii
I. INTRODUCTION	1
II. JUPITER DECAMETRIC RADIATION	3
A. Brief History of Decametric Observations and Articles	3
B. Characteristics	4
1. Average Spectrum	4
2. Periodicities	4
3. Burst Structure	6
4. Dynamic Spectra	7
5. Polarization Characteristics	8
6. Source Size	9
7. Power Output	9
III. TERRESTRIAL KILOMETRIC RADIATION	10
A. A Brief History of Terrestrial Kilometric Radiation Observations	10
B. Characteristics	10
1. Average Spectrum	10
2. Periodicities and Correlations	11
3. Burst Structure	12
4. Dynamic Spectra	12

	Page
5. Polarization Characteristics	13
6. Spin Modulation	13
7. Source Size and Location	13
8. Power Output	13
IV. EMISSION THEORIES AND OBSERVATIONAL CHECKS	14
A. Jupiter Decimetric Emission	14
1. Warwick's model	14
2. Ellis' model	14
3. Gledhill Model	15
4. Goldreich and Lynden-Bell [1969]	15
B. Terrestrial Kilometric Radiation	15
1. Perkins [1968]	15
2. Dunkel <u>et al.</u> [1970]	16
V. CONCLUSIONS	17
A. Summary of Observations	17
1. Average Spectrum	17
2. Periodicities	17
3. Burst Structure	17
4. Dynamic Spectra	18
5. Polarization Characteristics	18
6. Source Size and Location	18
7. Power	18
B. Discussion of Observations	18

	Page
C. Suggested Future Measurements	20
1. Jupiter	20
2. Earth	20
REFERENCES	22
TABLES	28
FIGURES	30

TABLE OF TABLES

	Page
TABLE 1 Summary of Magnitudes of Drift Rates	28
TABLE 2 Some Parameters of Jupiter's and Earth's Plasma . .	29

TABLE OF FIGURES

	Page
Figure 1 Average power spectrum of the radio emission from Jupiter. Square points are from Carr <u>et al.</u> [1964], triangles from McCulloch and Ellis [1966], and circles from various sources, as quoted by Roberts [1965]. (Figure from Carr and Gulkis, 1969.)	30
Figure 2 Histograms of occurrence probability as a function of CML for emission at 18 MHz and 10 MHz. The CML of the magnetic poles are indicated by vertical and dashed lines. (Figure from Carr and Gulkis, 1969.)	31
Figure 3 Probability of occurrence of 18 MHz radiation from Jupiter -- plotted as a function of both the System III longitude of the central meridian and the phase of Io relative to superior geocentric conjunction. The observations were made at the University of Florida Radio Observatory during the apparition of 1968-69. (Figure from Carr, 1970, slightly modified.)	32

- Figure 4 Emission beam structure proposed by Dulk
and others. (Figure from Carr, 1970,
slightly modified for reproduction.) 33
- Figure 5 Examples of source B frequency drifts as a
function of the location of Io and CML.
(Figure from Carr, 1970, after Dulk, 1965,
slightly modified for reproduction.) 34
- Figure 6 Decametric polarization as a function of radio
frequency and longitude. At low frequencies
variation of polarization with longitude becomes
nearly symmetric. (Figure is from Warwick,
1967.) 35
- Figure 7 This figure shows the spectral relationship of
the electric component of terrestrial kilometric
radiation to other phenomena. (Figure from
Gurnett, 1973.) 36
- Figure 8 Two consecutive frames demonstrating terrestrial
kilometric noise in the outputs of sweeping re-
ceivers with a spectrum extending from 45 kHz to
above 100 kHz in the lower graphs. The X axes are

calibrated in kHz and the Y axes in decibels below 1 gamma rms (i.e., 20 db represents 0.1 gamma), SEP refers to sun-earth-probe angle. LMT in Local Mean Time. Note that the frame took 18.4 sec. In this time there was very little change in spectrum. (Figure from Dunkel et al., 1970, modified slightly for reproduction.) 37

Figure 9 This figure shows what is believed to be terrestrial kilometric emission at 178 kHz and 100 kHz. Notice the dots (peak values) and the vertical bars (average values) as possible indication of spin modulation. 38

Figure 10 Occurrence of terrestrial kilometric noise versus L in earth radii and local mean time in hours for L based on Jensen-Cain field. Shading represents ratio of number of passes through each sector containing either terrestrial kilometric noise or broadband noise to total number of passes through that sector. Sectors marked by crosses, for which no data are available have been assigned the darkest shading appearing on two or more sides.

Noises occur predominantly in the dark hemisphere approaching lowest L shells near the midnight meridian. (Figure from Dunkel et al., 1970, modified for reproduction.) 40

Figure 11 Variation of the auroral electrojet index AE with respect to the time of occurrence of 32 broadband and highpass noise events. Mean AE nearest to time of events (0 hours) shows marked increase over those further removed in time. Little difference appears between data recorded at low L (< 11) and high L (> 11). (Figure from Dunkel et al., 1970.) 42

I. INTRODUCTION

The sun, the earth, and Jupiter are the only bodies in the solar system known to have magnetic fields. This paper is concerned with radio emissions which are believed to be consequences of Earth's and Jupiter's magnetic fields and trapped particles. Strong intermittent signals with possible continuous signals at a lower level in the 10 to 40 MHz range have been observed coming from near Jupiter. If magnetic fields are considered (see Table 2), possibly analogous emissions in the ~ 20 kHz to ~ 1 MHz range have been observed near the earth by satellite observations. To be consistent with the terminology used for the Jovian radio emission, we will refer to the terrestrial emission as "Terrestrial kilometric" radiation. The emphasis of this paper will be on reviewing the observations of the two phenomena with some discussion on possible generation theories.

There are many observational and review articles on the Jupiter decametric emission. The decametric emission shows complicated structure when viewed from Earth. This structure is due to the mechanisms of generation of the emission and due to the propagating characteristics of the Jovian and interplanetary plasmas. The observations of the terrestrial kilometric radiation (also called "highpass" noise by Dunkel) are at an early state. The few observations now published do not show a complicated structure like that of Jupiter.

However, there may be similarities between the low frequency (below 15 MHz) part of the Jovian decametric radiation and the terrestrial kilometric radiation.

It should be noted that Jupiter has a faster rotation rate than earth (factor $\sim 2 \frac{1}{2}$), a stronger magnetic field (factor ~ 30), and a greater gravitational acceleration (factor $\sim 2 \frac{1}{2}$). Modeling earth against Jupiter considering only the magnetic fields must be done with great caution especially when considering interactions with other bodies (including the solar wind) because of the greater inertial and gravitational effects on Jupiter's magnetosphere.

II. JUPITER DECAMETRIC RADIATION

A. A Brief History of Decametric Observations

The first observations of radio emission from Jupiter were made by Burke and Franklin [1955] at a frequency of 22.2 MHz. Subsequently, earlier records of Jovian emission at 18.3 MHz were found by Shain [1956] and a periodicity with central meridian longitude was observed. This periodicity was later found to be different from system II and the new system III was defined [Carr, et al., 1958]. In 1956, Burke and Franklin observed that the emission was most often right-hand circularly polarized. This polarization was the first evidence of Jupiter's magnetic field. Review papers by Roberts [1963] and Douglas [1964] include much of the background information available at the time. Decametric observations acquired a new dimension when Bigg [1964] discovered that many emissions from a source (called source B by Carr) are correlated with the location of Jupiter's moon Io. Later review papers by Ellis [1965], Warwick [1967], Carr and Gulkis [1969], and Warwick [1970] include this discovery and subsequent observations. Much material for this report has been drawn from these last three sources.

Hopefully, the observational data on Jupiter's fields and particles will take another quantum jump with direct probe measurements in the near future.

B. Characteristics

1. Average Spectrum

According to Carr and Gulkis [1969], the frequency of observed decametric radiation from Jupiter ranges from 3.5 MHz to 39.5 MHz (Figure 1) with an observed intensity ranging from $\sim 10^{-21}$ to $\sim 10^{-24}$ W M⁻² Hz⁻¹. This intensity is an average over active and inactive periods. Active periods may be ~ 10 times as intense as the average. The actual bursts which make up an active period may be 3 or 4 orders of magnitude greater in intensity than shown in Figure 1. The low frequency cutoff is believed due to Earth's ionosphere and the power spectrum below the cutoff is unknown.

2. Periodicities

Central Meridian Longitude -- According to Roberts [1963], emission between 15 MHz and 30 MHz recurs with a period of 9 hours 55 minutes 29.37 seconds. This defines system III longitude if its 0.0 time longitude coincides with system II longitude at 0.0 U. T. on 1 January 1957. The features of the emission pattern vary with frequency. At 18 MHz there are three peaks A, B, and C (Main, Early, and Late in Warwick's terminology) at central meridian longitudes (CML) $\sim 270^\circ$, $\sim 160^\circ$, $\sim 320^\circ$ respectively [Carr and Gulkis, 1969]. There is almost no activity in the vicinity of the CML of the southern magnetic pole ($\sim 20^\circ$) and a secondary minimum at the CML of the northern magnetic pole ($\sim 200^\circ$). The pole has a CML because the magnetic field inclined from rotation axis about 7° [Warwick, 1970]. However, at 10 MHz there is a maximum at the CML of the northern magnetic pole and

a fairly high level of activity at the CML of the southern magnetic pole. See Figure 2.

Io Effect -- Although much has been written about the modulating effect of Io on the emission from sources B and C at the higher frequencies (usually > 15 MHz), I will give only a brief summary. Kaiser et al. [1972] show with about 17 years of data that there is probably an Io-controlled storm every 12.95 hours. This is when Io sweeps past the same Jovian longitude. The two sources are then explained by Dulk [1967] as resulting from a thin hollow cone shaped beam originating from the point where the flux tube which passes through Io intersects the ionosphere. We see emissions when the edges of the cone intersect the earth. Figure 3 from Carr [1972] shows the pattern of emissions observed as a function of CML and Io position. Figure 4 shows the proposed emission beam structure.

Longer Periodicities -- Carr [1971] says that although Dulk and others imply all three main sources are due to the above beaming he believes most of Source A to be from a different sort of beaming which is dependent upon the Jovicentric declination of earth (D_E). This is supported by Kaiser et al. [1972] by showing a $12.0 \pm .2$ year periodicity which they say is consistent with the 11.9 year period for the Jovian year. Previously there had been some shorter term studies suggesting a correlation with the solar cycle [Gallet, 1961; Smith, Carr et al., 1965], but there seems to be considerable doubt thrown on these by Carr [1971] and Kaiser et al. [1972].

3. Burst Structure

L Bursts -- According to Douglas and Smith [1967] and others, the decametric storms are made up of groups of bursts which may last for several minutes. These groups have a bandwidth of less than 2 MHz [Gallet, 1961]. They are made up of pulses on the order of a second or longer (L bursts). Douglas and Smith [1962, 1967] observed the L bursts drifting in and out of simultaneity at different observing stations on earth with baselines on the order of 10 km to 100 km. From correlation considerations before and after Earth Jupiter oppositions, they conclude that most of the L bursts are due to scintillations in the interplanetary medium. This result seems to be accepted by others in the field notably Carr and Gulkis [1969] and Gordon and Warwick [1967].

S-Bursts -- Frequently at frequencies about 15 MHz the L bursts have superimposed shorter bursts, 0.1 second or shorter (S bursts or millisecond bursts in Warwick's usage). Riihimaa [1968a, b] and Baart, Barrow and Lee [1966a, b] found that bursts which are shorter 10 msec. are associated primarily with sources B and C and are presumed to be of Jovian origin. Flag et al. [1971] found these bursts can be as short as 8 - 10 microseconds measured with a receiver bandwidth limited to ~ 2 microseconds. S burst storms correlate with Io to a higher degree than storms not dominated by S bursts. Block et al. [1969] found the wave form of S bursts to correlate when observed at two stations with a baseline of 900 km. They also found phase shifts to correspond with wavefront geometry only. This tends to confirm the Jovian origin of the S-burst structure.

The S bursts tend to drift negatively with time. Paul and Carr [1969] measured the average drift rate (at 20 MHz) to be $-18.6 (+ 3.7)$ MHz/sec. When observed with a narrow band receiver this produces short pulses; in the case above they averaged 16.0 ± 2.2 msec. which implies a bandwidth of about 300 kHz. The Flag et al. [1971] wide band receiver found drift rates up to 10 GHz/sec. This high drift rate is probably not due to motion of particles in a field (an electron would need an energy \sim BeV).

4. Dynamic Spectra

The various sources seem to have different dynamic spectra. Before the Io control was discovered, Warwick [1963a, b] found dynamic spectra of storms showed features which reappeared on the same CML. Dulk [1965] found four distinct regions which depended on Io position with his fourth source being in a low intensity region ($\lambda_{1111} \sim 50^\circ$ and $\nu_{Io} \sim 100^\circ$) but identifiable by its narrow positive drifting spectrum. Sources A and C have characteristic spectra usually negative drifting. Source B was also very predictable with its positive drifting frequency which sometimes changes negative later. "The most striking feature of the dynamic spectra observed by Warwick and Dulk is the long thin arch which sometimes terminates an early source storm" [Gulkis and Carr, 1969]. It appears that the position, shape and maximum frequency is very sensitively related to Io's position [Warwick, 1967] (Figure 5).

The highest frequency observed was 39.5 MHz which Carr and Gulkis suggest is the maximum electron gyrofrequency in the emission region, possibly near the planet's surface.

Riihimaa [1968a, b] found a fine structure in decasecond bursts. Frequency versus time plots of the received signals showed diagonal bands (approximately 200 to 300 kHz in separation) which indicated frequency drift rates of about .1 MHz/sec. These patterns appear to be Io independent and the direction of the drift is usually dependent on the CML.

5. Polarization Characteristics

At higher frequencies (> 20 MHz) decametric radiation is predominantly righthand elliptically polarized at all longitudes [Barrow, 1964; Sherrill, 1965; Barrow and Morrow, 1968] and lefthand polarized at lower frequencies (< 10 MHz) according to Gulkis and Carr [1969]. They say most of the published data were based on the assumption of complete polarization. Sherrill [1965] found the polarization fraction to be at least .8 above 15 MHz so that this is a valid assumption to make at these frequencies. According to Warwick [1967] the stability of the elliptical polarization implies that the wave originated near the electron gyrofrequency. Warwick and Dulk [1964] found the major axis of the ellipse to be perpendicular to the projected field which Warwick [1967] says implies extraordinary mode of propagation.

6. Source Size

According to Carr and Gulkis [1969] the smallest incoherent source which would be resolved with the longest possible terrestrial baseline is ~ 100 km. Dulk [1970] reports that with a long baseline interferometer (487000λ at 34 MHz) he found the upper limit for an incoherent source to be $\sim 0.1''$ or ~ 400 km. This upper limit has been confirmed by other groups [Brown, Carr, Block, 1968; Carr *et al.*, 1970; Lynch *et al.*, 1972]. None of these experiments have resolved the source or precisely located it. All of these measurements have all been at frequencies higher than 18 MHz.

7. Power Output

In order to estimate the power output of an event one must know or make assumptions about the received signal strength, the distance to the source and the beam pattern. In the case of Jupiter, the beam pattern is the primary point of question. Assuming a 5° cone vertex angle in a right circular cone and a 10 MHz bandwidth, Warwick [1967, 1970] gets a typical total power $\sim 2 \times 10^8$ watts. He notes that different assumptions yield values like 10^7 watts for a narrower cone and 10^{11} watts for a hemispherical beam.

Since the low frequency component of the decametric emission has different characteristics, it may be useful to estimate a total power for it. An assumption of 15 MHz bandwidth, an observed intensity of $2 \times 10^{-22} \text{ W m}^{-2} \text{ Hz}^{-1}$ [May and Carr, 1969; Dulk and Clark, 1966], and a spherical emission pattern yields power $\approx 1 \times 10^{10}$ W. An assumption of 10 MHz bandwidth and a solid pencil beam 40° in longitude and 12° in latitude yields power $\approx 2 \times 10^8$ W.

III. TERRESTRIAL KILOMETRIC RADIATION

A. A Brief History of Terrestrial Kilometric Radiation Observations

Dunkel, Ficklin, Rorden and Helliwell reported in 1970 the discovery of two previously unreported phenomena, "Broadband" noise and "Highpass" (kilometric) noise. Observed with OGO 1 broadband noise is thought by Dunkel et al. to be a non-propagating local disturbance in the vicinity of the satellite. The kilometric emission has a low frequency cutoff always higher than 20 kHz and appears to have an origin distant from the satellite. There have been observations by Gurnett of these kilometric emissions up to 178 kHz. A paper presented by Stone [1971] reported kilometric emissions up to ~ 1 MHz with a maximum intensity at ~ 300 kHz.

B. Characteristics

1. Average Spectrum

According to Dunkel et al., kilometric noise is characterized by a continuous spectrum from the low frequency cutoff up to above 100 kHz: the limit of their receivers. The author has received figures from Dr. Gurnett [1973] which show emissions he believes to be the same as Dunkel's highpass noise at 100 kHz and 178 kHz. Its spectral relation to other phenomena is shown in Figure 7. Figure 8 shows two frames of Dunkel's data. Dunkel interprets the low frequency cutoff as a propagation cutoff on the path between the source and the

receiver. He expects the cutoff to be at the electron plasma frequency and finds that local electron density corresponds to an electron plasma frequency at about $1/5$ of the observed cutoff. Notice that in Gurnett's Figure 9, the emission is above the upper hybrid resonance noise.

2. Periodicities and Correlations

Location -- On Jupiter's decametric emissions, the study of periodicities tell us something about the conditions necessary for emission, beaming, and possibly about the location of the source. No such periodicities have been noticed in the study of highpass except for the period of the observing satellite itself (i.e., its location). According to Dunkel et al., kilometric noise occurs mainly at night in a region that lies closest to earth at local midnight (see Figure 10). Although Figure 10 goes only to $L = 11$, the noise has been observed out to 24 earth radii and appears mainly on the nightside. Gurnett has similar diagrams from IMP-I.

Broadband -- Dunkel reports that kilometric noise tends to occur in conjunction with another wideband (0.3 - 100 kHz) noise which appears to be local to the satellite. "Broadband" noise shows no cutoff at electron gyrofrequency, but does show spin modulation. Spin modulation is surprising because the orientation of the magnetic antenna is unchanged by rotation of OGO-1. This suggests that the satellite itself may be involved in the generation of broadband noise.

Magnetic Latitude -- Dunkel reports most kilometric emission events are detected between 20° and 40° N. The observed locations may be limited to the orbit of the satellite.

Altitude -- Dunkel reports events have been detected from within one earth radius in L value to the plasmapause out to and past the mean position of the magnetopause.

Magnetic Activity -- Dunkel shows a close relationship between kilometric emissions and the auroral electrojet index AE. The AE index represents the difference in gammas between the measured hourly maximum and minimum variations of the H field measured on the ground in the auroral zone. He states that for four events studied each event was preceded within 2 minutes by micropulsations with periods on the order of 2 minutes.

3. Burst Structure

Dunkel defines a burst as a set of consecutive frames showing highpass noise preceded and followed by at least one frame with no detectable noise. He says the mean length is 23 minutes with a range from 1 minute to 5.9 hours. Gurnett's Figure 9 shows some rapid fluctuation (less than 12 seconds) in the peaks and averages representation.

4. Dynamic Spectra

Both Dunkel and Gurnett's data show no fast dynamic spectra changes. Sequential frames of Dunkel's data, however, often show the low cutoff to start at a high frequency, descend to a minimum and then rise before the burst ends. The minimum varies with satellite position. One example: 90 kHz at $3.9 R_E$ to 50 kHz at $5.4 R_E$. With magnetic latitude and local mean time approximately constant at 34° and 23 hours.

5. Polarization Characteristics

As far as I know, none have been measured.

6. Spin Modulation

Dunkel reports to have found no spin modulation. This is not surprising since the magnetic antenna is aligned to be sensitive along the axis of rotation of the satellite OGO 1. Gurnett's IMP-I data in Figure 9, however, do show some spin modulation. The vertical lines in the data are computed averages over a satellite spin period and the dots represent the peak value during that time.

7. Source Size and Location

Stone [1971] has analyzed spin modulation data and found the source to be very close to earth and smaller than the size of earth. The correlation with AE index suggests that the source may be near the auroral region.

8. Power Output

Dunkel reports the geometric mean of the maximum power densities of all bursts is $3 \times 10^{-14} \text{ Wm}^{-2} \text{ Hz}^{-1}$. In the $L = 5$ region this is comparable to whistler-mode noise. However, since the location of the source, the emission pattern and the full spectral range are not known, the total output power has not been calculated. The author's upper limit estimation of average power is a maximum $\sim 10^8 \text{ W}$ assuming spherical emission pattern at 10 earth radii with a 1 MHz bandwidth. A lower limit is calculated by assuming a beam which looks like a strip from 20° to 40° north latitude on the nightside of Earth only. A lower limit on the power of 2.7×10^6 watts is estimated.

IV. EMISSION THEORIES AND OBSERVATIONAL CHECKS

For both Jupiter decametric emission and earth kilometric emission there are a number of different possible mechanisms. In most cases there are observational checks which could be made in the near future. I will very briefly outline some of the theories and possible checks.

A. Jupiter Decametric Emission

1. Warwick's Model

Theory -- Electron gyrofrequency emissions from the active region (L values between 2 and 3 Jupiter radii) propagate along magnetic field lines, bounce off of Jupiter's ionosphere, and propagate outward in a pencil shaped beam at a large angle to the magnetic field lines.

Objections -- $Y = 1$ stop band for emissions generated at $Y > 1$ [Ellis, 1965].

Checks -- Theory depends on "grossly displaced dipole" magnetic field which can be checked with a fly-by magnetometer.

2. Ellis' Model

Theory -- Helical electron beams emit Doppler shifted cyclotron radiation. The Io control is effected by hydromagnetic or electromagnetic waves from a distance.

Objections -- Self inconstancy; wave grows too large and violates physical basis of dispersion relation [Warwick, 1970].
Observational; predicted details of dynamic spectra conflict with observed dynamic spectra [Warwick, 1970].

Checks -- Required electron density and energy at one R_J could be checked with fly by.

3. Gledhill Model

Theory -- Io generates waves locally at plasma frequency.

Objection -- Requires very high plasma density which may be self inconsistent [Carr, 1969].

Check -- Plasma density can be checked with sounding experiment on a fly by.

4. Goldreich and Lynden-Bell [1969]

Theory -- Io drags flux tube through ionosphere. Io has an induced voltage which drives current through flux tube and dissipates $\sim 5 \times 10^{11}$ W at each foot. Coherent cyclotron radiation produced by current carrying electrons at decametric frequencies is at right angles to magnetic field lines.

Checks -- Requires specific electron momentum distribution which could be measured.

B. Terrestrial Kilometric Radiation

1. Perkins [1968]

Theory -- Monoenergetic electrons ($E \sim 10$ keV) are computed to make auroral zone topside plasma unstable to electrostatic plasma

waves close to upper hybrid resonance.

Objection -- According to Dunkel et al. the electrostatic waves need to be converted to electromagnetic to propagate to satellite.

Check -- Plasma instabilities can be detected with radar scatter experiment and correlated with satellite detection of kilometric radiation. This experiment is described in Perkins [1968].

2. Dunkel et al. [1970]

Theory -- Cyclotron radiation generated close to earth.
Propagation assumed confined to field lines (in region of generation).

Objection -- Observed power spectral density too high by factor 10^4 .

Check -- 1. More observations to discover the beaming characteristics may provide test of confinement to field lines and cutoff characteristics.

V. CONCLUSIONS

A. Summary of Observations

1. Average Spectrum

The highest Jovian decametric frequency observed is about 40 times higher than the highest terrestrial kilometric emission frequency observed. The maximum intensity of the low-frequency decametric emission is around 10 MHz. The maximum intensity for kilometric radiation is around ~ 300 kHz. The scale factor is about 33. Jupiter's magnetic field is about 30 times as strong as Earth's.

2. Periodicities

There is apparently nothing similar to Io-control of decametric emission in the phenomenology of the terrestrial kilometric emission. Since at low frequencies (below 15 MHz) the Jupiter decametric emission shows very little Io control, there may be a basis for comparison with the terrestrial kilometric emission. The 11.9 year period in the low frequency radiation according to Carr [1969] indicates a beam width which is sensitive to angle changes of 3° from the equatorial plane.

3. Burst Structure

There is apparently nothing similar in the terrestrial kilometric emission to the S burst structure typical of the Io-controlled

storms. However, the low frequency decametric emissions have a continuous nature similar to terrestrial kilometric emission.

4. Dynamic Spectra

There is nothing similar in the terrestrial kilometric data to the Io control of the Jovian decametric dynamic spectra.

5. Polarization Characteristics

The decametric emission is predominately elliptically polarized. The polarization of the terrestrial kilometric emission has not been determined.

6. Source Size and Location

The source of the decametric radiation is smaller than 400 km at frequencies as low as 18 MHz. The terrestrial kilometric emission source size is implied to be 1 earth radius or less in diameter.

7. Power

The average power of the lower frequency Jovian decametric emission is probably at least 2×10^8 watts, but not above around $\sim 10^{11}$ watts. The average power of the earth kilometric events is probably at least on the order of $\sim 3 \times 10^6$ watts, but not above $\sim 10^8$ watts.

B. Discussion of Observations

A question of interest is "Can Jupiter decametric radiation and terrestrial kilometric emission have similar emission mechanisms?" Considering only the non Io-controlled emissions, it is possible that similar mechanisms are involved.

The Jovian decametric emission appears to be generated near the gyrofrequency. The gyrofrequency is indicated by the elliptical polarization observed and the stability of the spectrum. Above the ionosphere Jupiter's plasma frequency is much lower than the gyrofrequency for regions with gyrofrequencies corresponding to decametric wavelength radiation (Table 2). This allows frequencies slightly above the gyrofrequency to propagate because the upper hybrid resonance is approximately equal to the gyrofrequency.

In the earth's magnetosphere the plasma frequency is generally above the gyrofrequency (Table 2 -- the plasma densities shown may be a little high according to Gurnett). However, the plasma density is lower than usual on the nightside of earth, in the polar regions (due to the tendency of plasma density to follow magnetic lines of force), and where the plasma is depleted by auroral arcs. If the plasma density is low enough the plasma frequency may be enough lower than the gyrofrequency to have an emission at the gyrofrequency Doppler shifted above the upper hybrid frequency. The kilometric emission is observed away from the equator on the nightside of Earth, and shortly after AE index increases. The AE index increase may indicate massive depletion of electrons by auroral arcs of a region near the magnetic detectors. That both the Jovian decametric and terrestrial kilometric emissions are magnetically controlled is further suggested by the scaling of the maximum gyrofrequencies (ratio ~ 30) and the observed spectra (ratio ~ 40).

If Earth's kilometric emission does come from regions described above and near the gyrofrequency, we should find that the emissions

come from small regions primarily near auroral zones and that the emissions are elliptically polarized. Stone [1971] indicated the size and location required is possible. The polarization has not been measured. Future experiments are suggested in the next part of this section.

C. Suggested Future Measurements

1. Jupiter

- a. Plasma density in vicinity of Jupiter including inside the orbit of Io with a fly-by experiment.
- b. Electron energy spectrum in the same area.
- c. Magnetic field shape, strength, and polarity in the same area.
- d. Decametric emission spatial patterns.

2. Earth

- a. Polar orbit observations at various altitudes of kilometric emission to check spatial patterns and polarization characteristics.
- b. Check of present data for periodicities and correlations with various phenomena including AE, solar wind fluctuations, and the position of the moon.
- c. Wideband satellite observations to look for fine structure similar to diagonal bands in decametric data.
- d. Satellite observations at higher frequencies to determine emission characteristics.

- e. Poynting flux measurements to determine location and other characteristics of source.
- f. Spin modulation studies for same reason as e. (Some of these are being done.)
- g. A determination of total power output could be made if the whole spectrum and beaming characteristics were determined.

REFERENCES

- Al' Pert, YA. L., VLF and ELF waves in the near-Earth plasma, Spa. Sci. Rev. 6, 781, 1967.
- Baart, E. E., C. H. Barrow, and R. T. Lee, Burst structure of Jupiter's decametric radiation, Astron. J., 71, 377, 1966 (abstract).
- Baart, E. E., C. H. Barrow, and R. T. Lee, Millisecond radio pulses from Jupiter, Nature, 211, 808, 1966b.
- Barrow, C. H., Polarization observations of Jupiter at decameter wavelength, Icarus, 3, 66, 1964.
- Barrow, C. H., and D. P. Morrow, The polarization of the Jupiter radiation at 18 Mc/s, Ap. J., 152, 593, 1968.
- Bigg, E. K., Periodicities in Jupiter's decametric radiation, Planet. Spa. Sci., 14, 741, 1966.
- Block, W. F., M. P. Paul, T. D. Carr, G. R. Tebo, and V. M. Robertson, unpublished, 1969 (summarized in Carr and Gulkis, 1969).
- Burke, B. F., and K. L. Franklin, Observations of a variable radio source associated with the planet Jupiter, J. Geophys. Res., 60, 213, 1955.

Burke, B. F., and K. L. Franklin, Carnegie Institute of Washington Year Book, 74, 1956.

Burke, B. F., Planets and Satellites, University of Chicago Press, 1961.

Carr, T. D., A. G. Smith, H. Bollhagen, N. F. Six, and N. E. Chatterton, 18-megacycle observations of Jupiter in 1957, Ap. J., 127, 274, 1958.

Carr, T. D., A. G. Smith, H. Bollhagen, N. F. Six, and N. E. Chatterton, Recent decameter-wave-length observations of Jupiter, Saturn, and Venus, Ap. J., 134, 105, 1961.

Carr, T. D., and S. Gulkis, The magnetosphere of Jupiter, Annual Rev. Astro. and Astrophys., 7, 577, 1969.

Carr, T. D., Information from Jupiter's decametric radiation, NASA TM 33-543, 1971.

Davis, T. N., and M. Sugiura, Auroral electrojet activity index AE and its universal time variation, J. Geophys. Res., 71, 785, 1966.

Davis, T. N., and Y. S. Wong, UAG R-198, 1967.

Douglas, J. N., and H. J. Smith, Presence and correlation of fine structure in Jovian decametric radiation, Nature, 192, 741, 1961.

Douglas, J. N., Decametric radiation from Jupiter, IEEE Trans. MIL-8, 173, 1964.

Douglas, J. N., and H. J. Smith, Interplanetary scintillation in Jovian decametric radiation, Ap. J., 148, 885, 1967.

Dulk, G. A., Science, 148, 1585, 1965 (summarized in Warwick, 1967).

Dulk, G. A., Apparent changes in the rotation rate of Jupiter, Icarus, 7, 173, 1967.

Dulk, G. A. (Private communication to Warwick), 1968.

Dulk, G. A., Characteristics of Jupiter's decametric radio source measured with arc-second resolution, Ap. J., 159, 671, 1970.

Dulk, G. A., T. A. Clark, Almost continuous radio emission from Jupiter at 8.9 and 10 MHz, Ap. J., 145, 945, 1966.

Dunkel, N., and R. A. Helliwell, Whistler-mode emissions on the OGO-1 satellite, J. Geophys. Res., 74(26), 6371, 1969.

Dunkel, N., B. Ficklin, J. Rorden, and R. A. Helliwell, Low-frequency noise observed in the distant magnetosphere with OGO-1, J. Geophys. Res., 75, 1854, 1970.

Ellis, G. R. A., The decametric radio emission of Jupiter, Radio Sci., 69D, 1513, 1965 (summarized in Carr and Gulkis, 1967).

Flagg, R. S., G. R. Lebo, D. L. Sonoleny, Jupiter's decametric micro-pulse structures, Bull. Am. Phys. Soc. II, 15, 203, 1970 (abstract).

Gallet, R. M., Planets and Satellites, University of Chicago Press, 1961.

Gurnett, D. A., (private communication to N. D. Hosford), 1973.

Helliwell, R. A., Whistlers and Related Ionospheric Phenomena, Stanford University Press, 1965.

Kaiser, M. L., J. K. Alexander, Periodicities in Jupiter's decametric emission, Astrophys. Lett., 14, 1972.

Liemohn, H. B., Wave propagation in the magnetosphere of Jupiter, NASA TM33-543

Meyer, C. H., Planets and Satellites, University of Chicago Press, 1961.

May, J., T. D. Carr, Flux density measurements of the Jovian radiation below 10 Mc/s, Publicaciones No. 6, Departamients de Astronomia, Universidad de Chile, 187, 1969.

- Paul, M. P., and T. D. Carr, (unpublished, summarized in Gulkis and Carr, 1969), 1969.
- Roberts, J. A., Radio emission from the planets, Pla. Spa. Sci., 11, 221, 1963.
- Riihimaa, J. J., Structured events in the dynamic spectra of Jupiter's decametric radio emission, Astron. J., 73, 265, 1968a.
- Riihimaa, J. J., Spectra of Jovian millisecond pulses, Nature, 218, 1141, 1968b.
- Shain, C. A., 18 Mc/sec radiation from Jupiter, Aus. J. Phys., 9, 61, 1956.
- Sherrill, W. M., Polarization measurements of the decameter emission from Jupiter, Ap. J., 142, 1171, 1965.
- Smith, A. G., G. R. Lebo, N. F. Six, and T. D. Carr, Decameter-wavelength observations of Jupiter: The apparitions of 1961 and 1962, Ap. J., 141, 457, 1965.
- Stone, R. G., G. Fainberg, and L. W. Brown, Observations of traveling solar radio bursts, Paper SC9 Fall AGU Meeting, San Francisco, 1971.

Warwick, J. W., Dynamic spectra of Jupiter's decametric emission, 1961,
Ap. J., 137, 41, 1963a.

Warwick, J. W., Position and sign of Jupiter's magnetic moment, Ap. J.,
137, 1963b.

Warwick, J. W., Radiophysics of Jupiter, Spa. Sci. Rev., 6, 841, 1967.

Warwick, J. W., Particles and Fields Near Jupiter, NASA CR-1685, 1970.

TABLE 1

Summary of Magnitudes of Drift Rates

Storm as a whole [Warwick 1967, Dulk 1965]	$\sim .001$ MHz/sec.
L burst diagonal bands [Riihimaa 1968]	$\sim .1$ MHz/sec. (changes sign at CML 150°)
S burst drift rates [Paul and Carr 1964]	~ 10 MHz/sec.
[Flag <u>et al.</u> 1971]	~ 1 GHz/sec.

TABLE 2

Some Parameters of Jupiter's and Earth's Plasmas

JUPITER (Ioannidis and Brice model along equatorial plane)

Distance	B_0 (gauss)	N_0 (m^{-3})	f_{pe} (MHz)	f_{ge} (MHz)
$\ll 1 R_J$	~ 10	$\sim 10^{-2}$	$\sim 9 \times 10^{-4}$	29
$1 R_J$	~ 1	$\sim 3 \times 10^{-2}$	$\sim 1.6 \times 10^{-3}$	2.9
$6 R_J$	$\sim 5 \times 10^{-2}$	~ 10	$\sim 2.8 \times 10^{-2}$	1.4×10^{-1}
$10 R_J$	$\sim 10^{-2}$	~ 30	$\sim 4.8 \times 10^{-2}$	2.9×10^{-2}
$22 R_J$	$\sim 10^{-3}$	~ 3	$\sim 1.6 \times 10^{-2}$	2.9×10^{-3}

EARTH (equatorial plane)

Distance	B_0 (gauss)	N_0 (cm^{-3})	f_{pe} (KHz)	f_{ge} (KHz)
300 km	4.5×10^{-1}	10^6	9000	1300
$1 R_e$	1×10^{-1}	5×10^3	640	290
$2.2 R_e$	1.5×10^{-2}	10^3	235	41
$3.2 R_e$	1×10^{-2}	2×10^2	130	29
$6.5 R_e$	2×10^{-3}	50	64	53
$18 R_e$	5×10^{-4}	10	28	1.4

Material in Table is based on Liemohn, H. B. [1972] and Al'Pert, Ya. L. [1967].

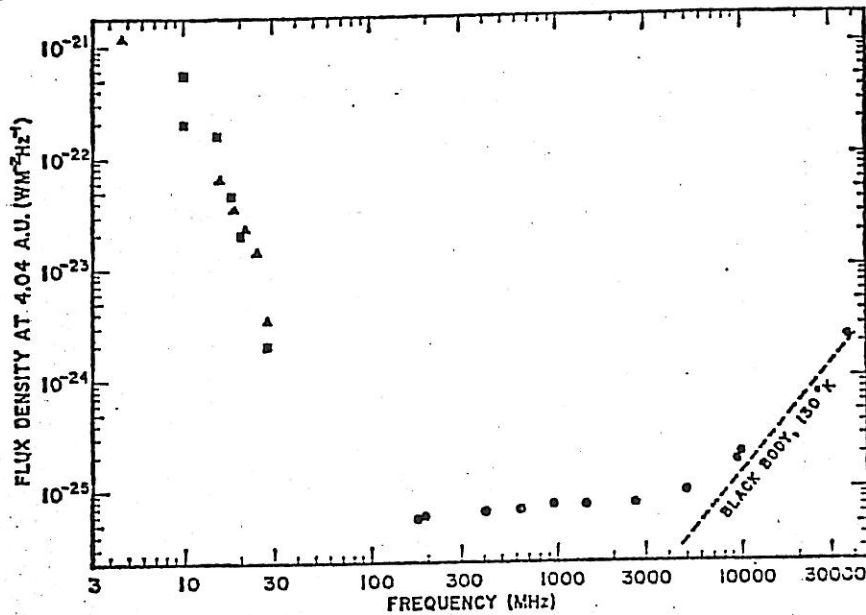


Figure 1 Average power spectrum of the radio emission from Jupiter.

Square points are from Carr et al. [1964], triangles from McCulloch and Ellis [1966], and circles from various sources, as quoted by Roberts [1965]. (Figure from Carr and Gulkis, 1969.)

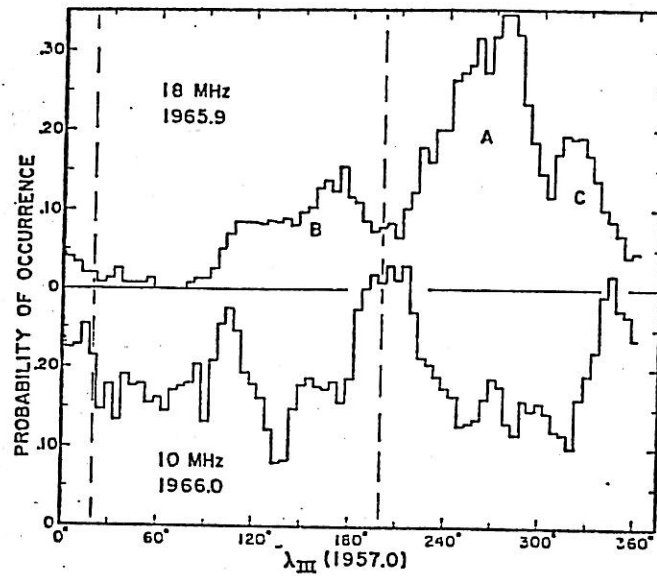


Figure 2 Histograms of occurrence probability as a function of CML for emission at 18 MHz and 10 MHz. The CML of the magnetic poles are indicated by vertical and dashed lines. (Figure from Carr and Gulkis, 1969.)

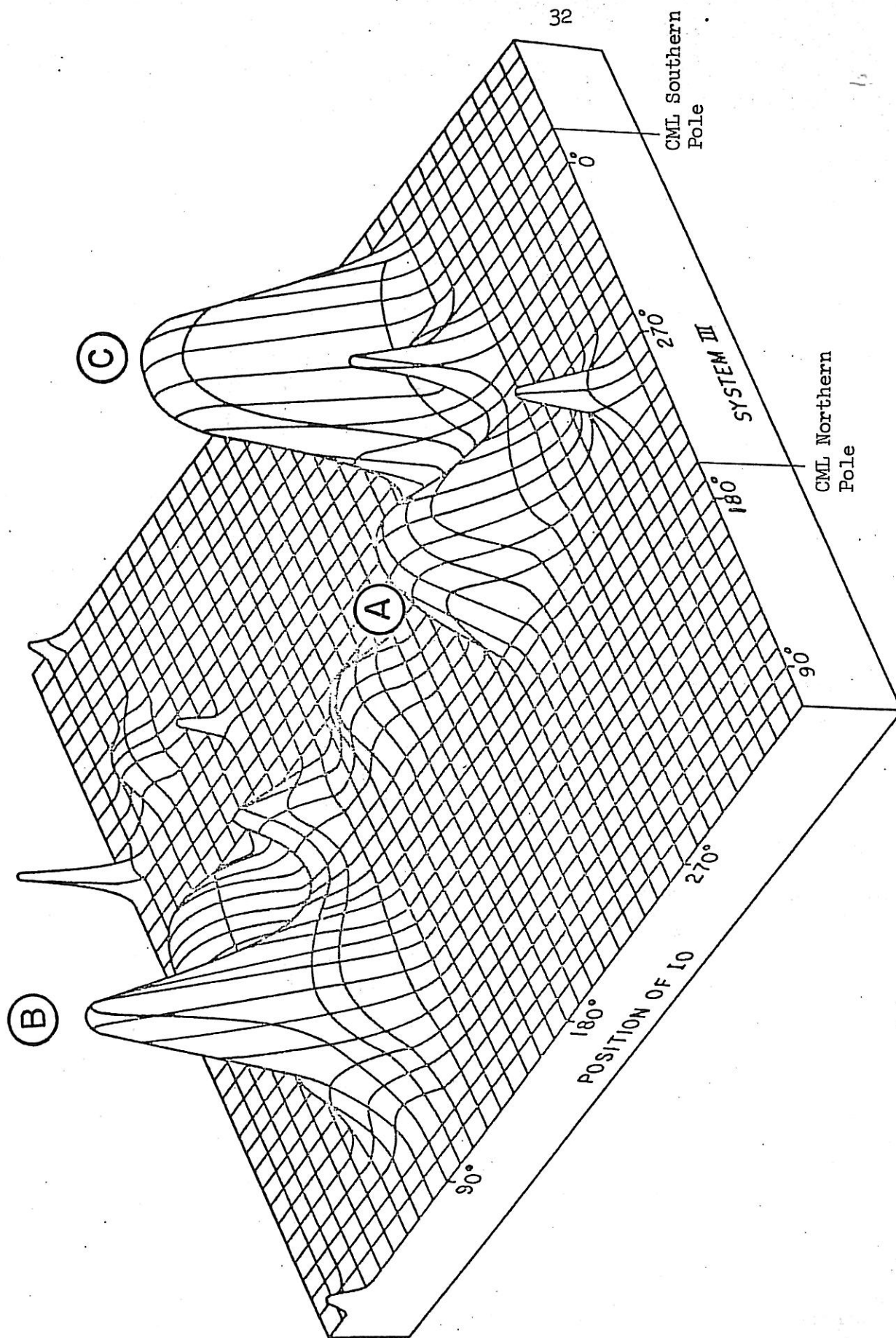


Figure 3 Probability of Occurrence of 18 MHz Radiation from Jupiter -- plotted as a function of both the System III longitude of the central meridian and the phase of Io relative to superior geocentric conjunction. The observations were made at the University of Florida Radio Observatory during the apparition of 1968-69. (Figure from Carr, 1970, slightly modified.)

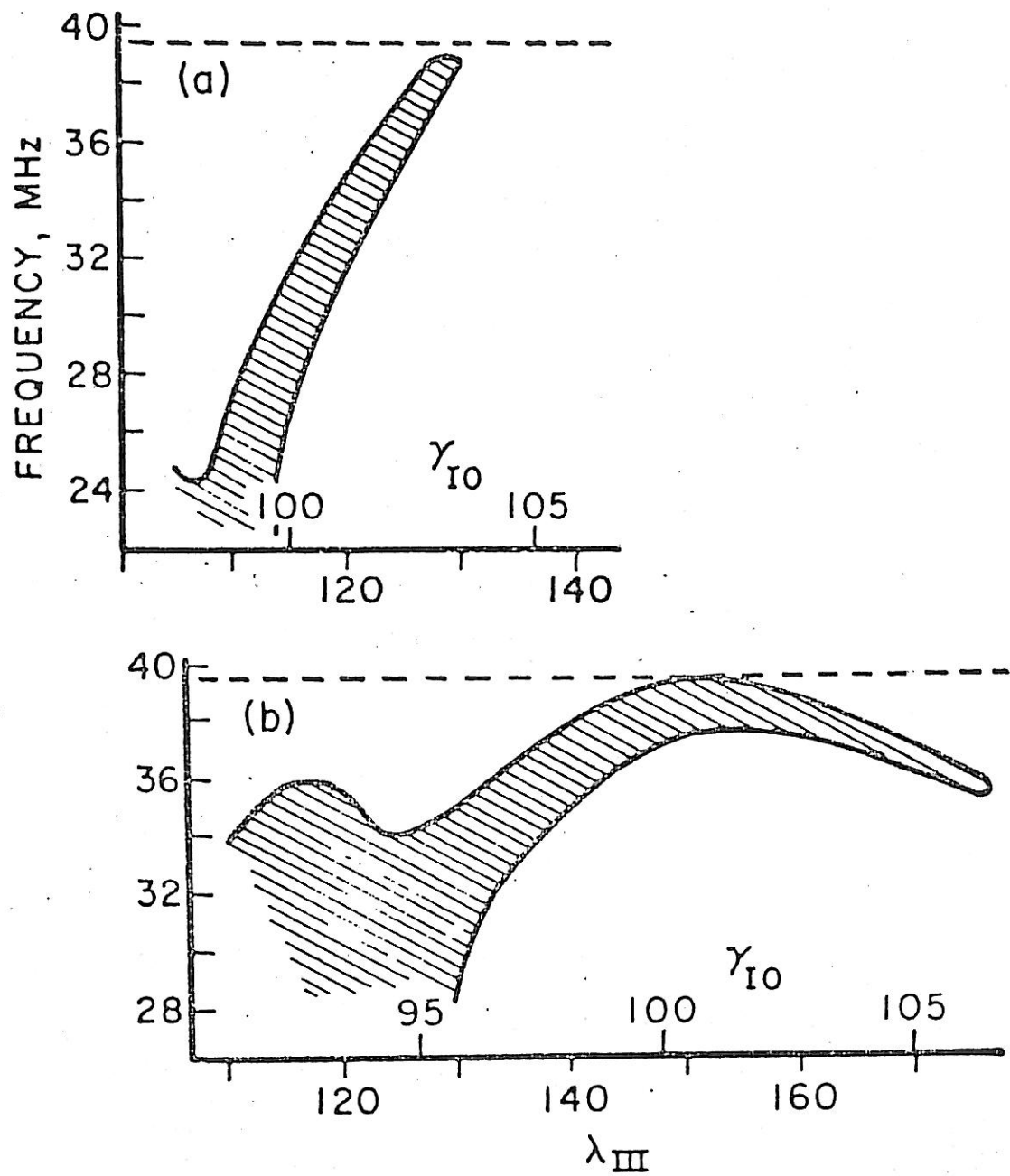


Figure 5 Examples of source B frequency drifts as a function of the location of Io and CML. (Figure from Carr, 1970 after Dulk, 1965, slightly modified for reproduction.)

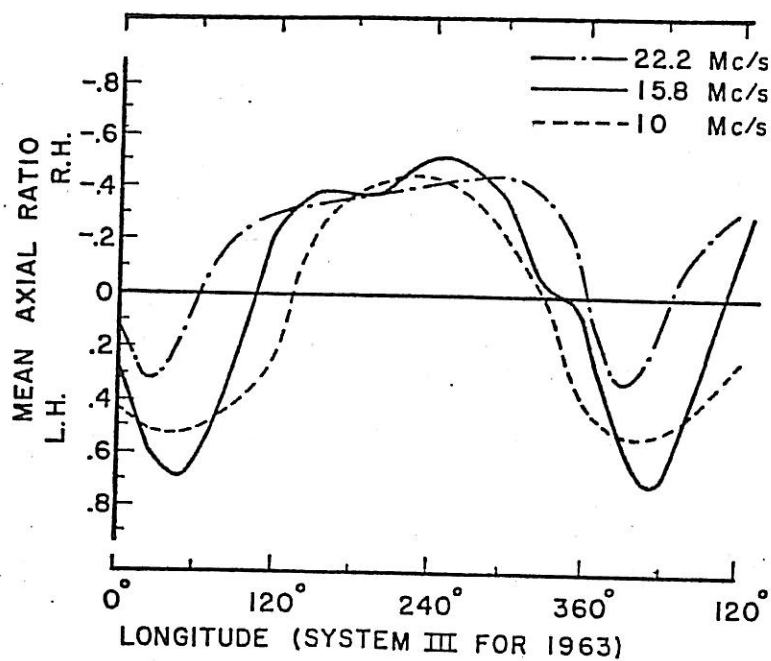


Figure 6 Decametric polarization as a function of radio frequency and longitude. At low frequencies variation of polarization with longitude becomes nearly symmetric. (Figure is from Warwick, 1967.)

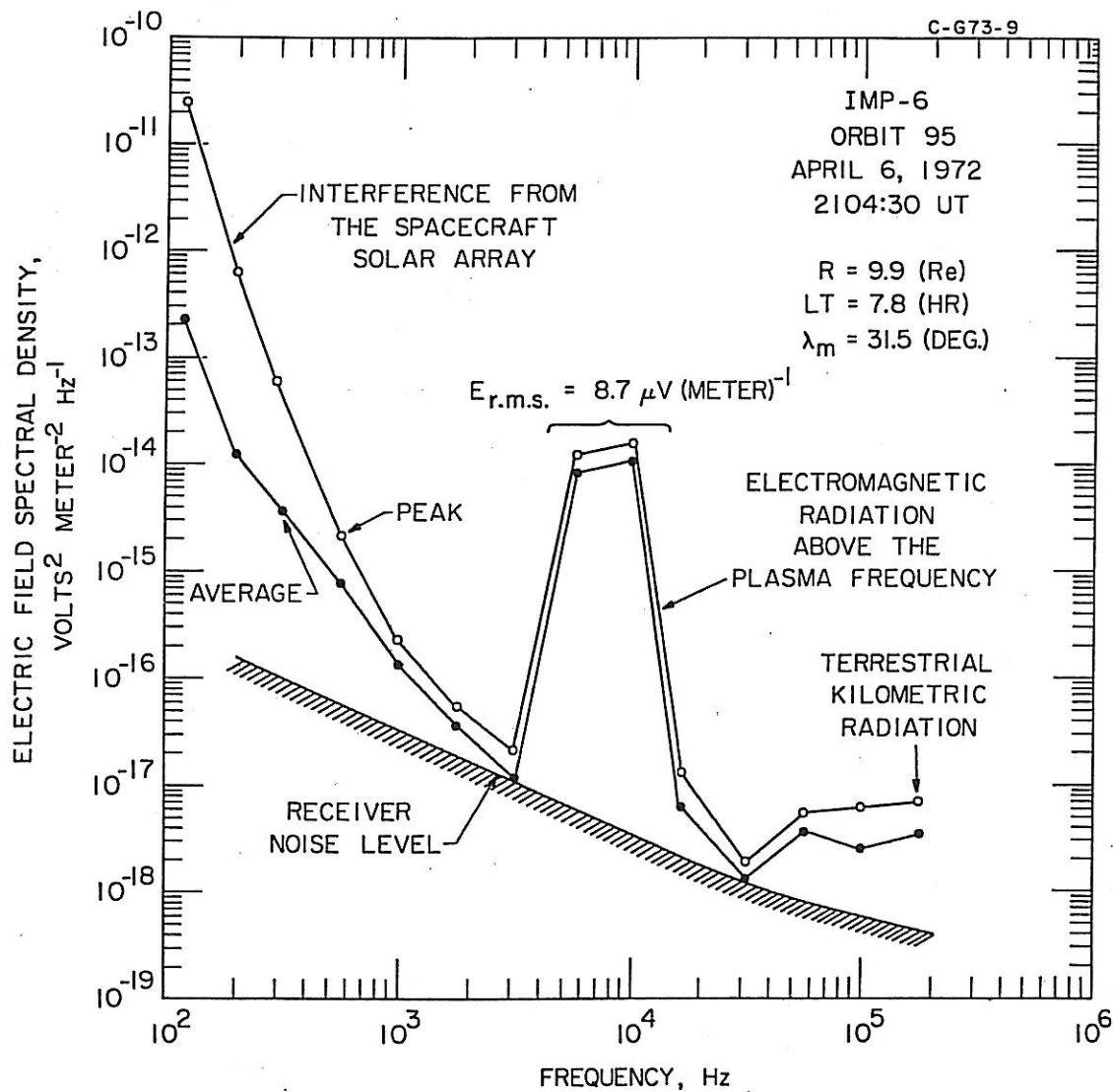


Figure 7 This figure shows the spectral relationship of the electric component of terrestrial kilometric radiation to other phenomena. (Figure from Gurnett, 1973.)

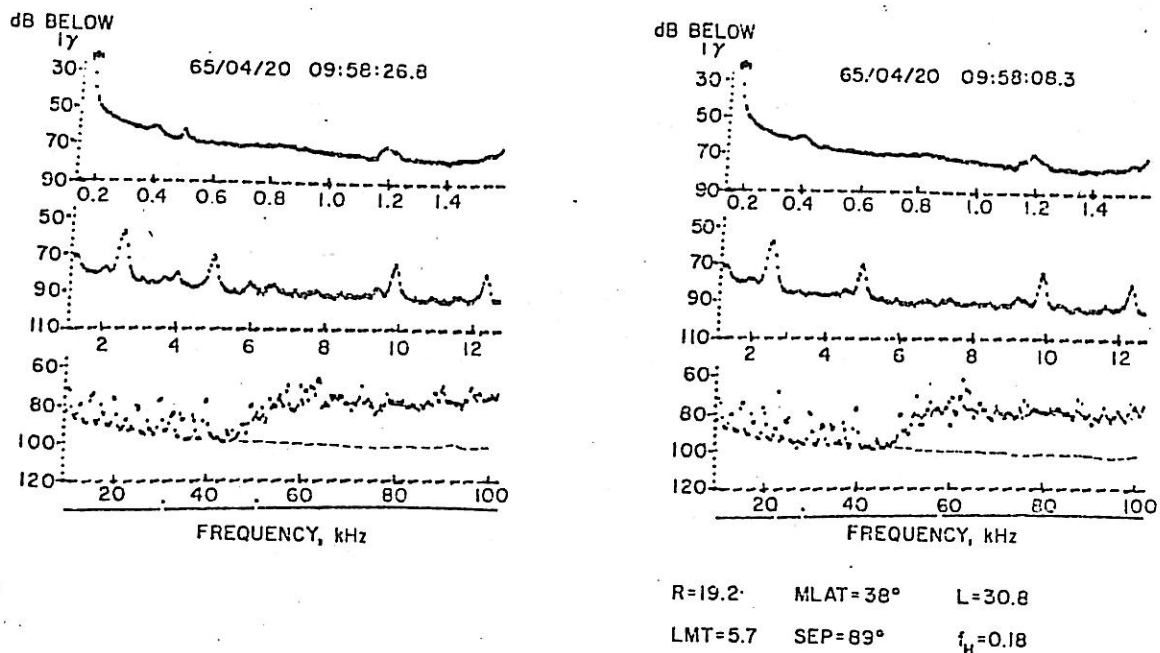


Figure 8 Two consecutive frames demonstrating terrestrial kilometric radiation in the outputs of sweeping receivers with a spectrum extending from 45 kHz to above 100 kHz in the lower graphs. The X axes are calibrated in kHz and the Y axes in decibels below 1 gamma rms (i.e., 20 db represents 0.1 gamma) SEP refers to sun-earth-probe angle. LMT is Local Mean Time. Note that the frame took 18.4 sec. In this time there was very little change in spectrum. (Figure from Dunkel et al., 1970, modified slightly for reproduction.)

Figure 9 This figure shows what is believed to be terrestrial kilometric emission at 178 kHz and 100 kHz. Notice the dots (peak values) and the vertical bars (average values) as possible indication of spin modulation.

B-673-8

IMP-6, ORBIT 61, NOV. 17, 1971

UPPER HYBRID RESONANCE NOISE → ELECTROMAGNETIC RADIATION ABOVE THE PLASMA FREQUENCY

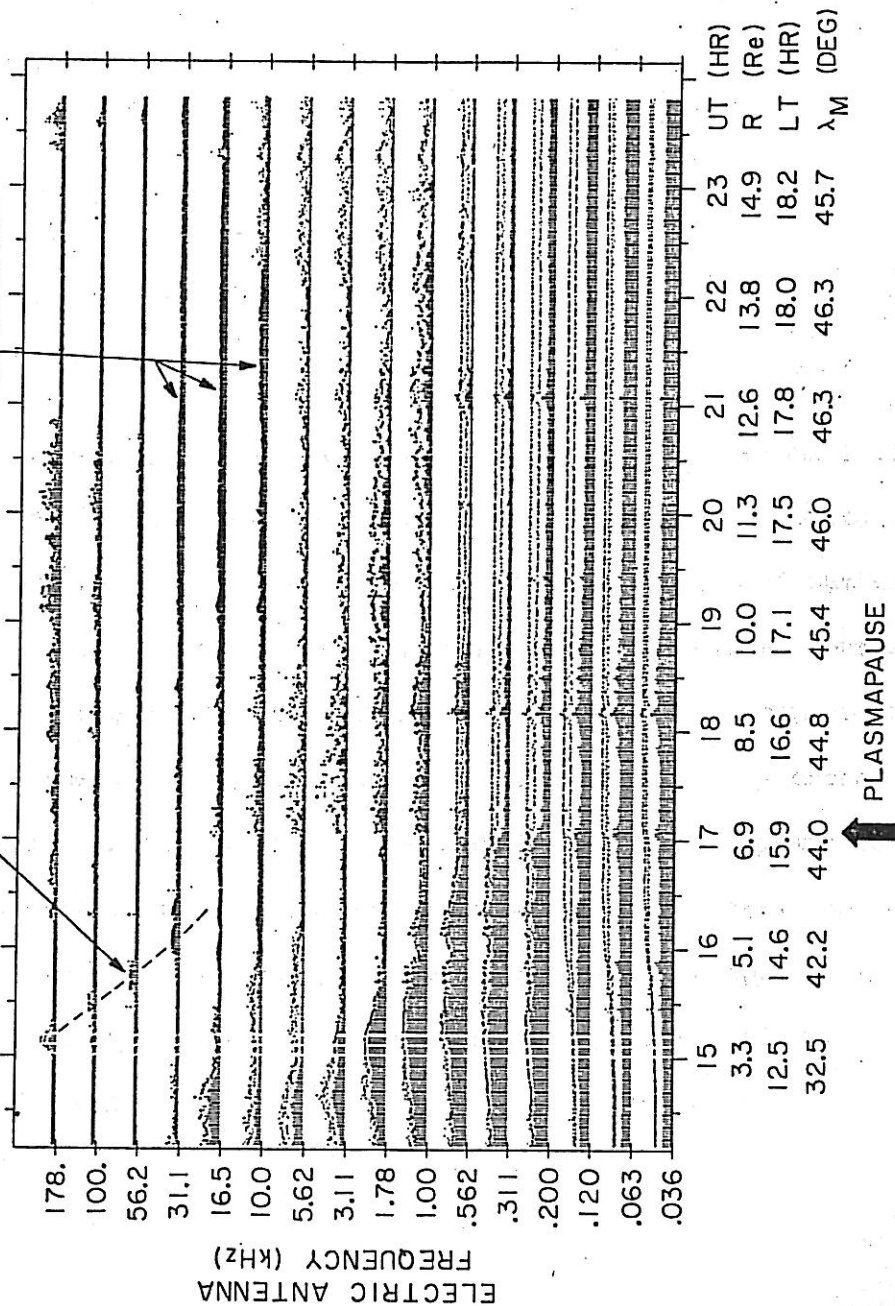


Figure 9

Figure 10 Occurrence of terrestrial kilometric noise versus L in earth radii and local mean time in hours for L based on Jensen-Cain field. Shading represents ratio of number of passes through each sector containing either terrestrial kilometric noise or broadband noise to total number of passes through that sector. Sectors marked by crosses, for which no data are available have been assigned the darkest shading appearing on two or more sides. Noises occur predominantly in the dark hemisphere approaching lowest L shells near the midnight meridian. (Figure from Dunkel et al., 1970, modified for reproduction.)

